Supporting Information

Polydopamine-Graphene Oxide Derived Mesoporous Carbon Nanosheets for Enhanced Oxygen Reduction

Konggang Qu, Yao Zheng, Sheng Dai, and Shi Zhang Qiao**

School of Chemical Engineering, The University of Adelaide, Adelaide, SA, 5005, Australia
Corresponding authors: s.dai@adelaide.edu.au; s.qiao@adelaide.edu.au

Experimental Section

Preparation of Graphene Oxide (GO): Graphite flakes were oxidized using the improved Hummers' method. Graphite (3 g) was added into a mixture of concentrated H_2SO_4/H_3PO_4 (360:40 mL), followed by the addition of $KMnO_4$ (18 g). The reaction mixture was heated to 50 ^oC and stirred for 12 h. The reaction was then cooled to room temperature and poured in ice water (ca. 400 mL) with the addition of H_2O_2 (30 %, 20 mL). The mixture was filtered over a PTFE membrane with a 0.45 μm pore size and washed with 200 mL of water, 200 mL of 30 % HCl, and 200 mL of ethanol (2×).

Exfoliation of graphite oxide to graphene oxide (GO) sheets was achieved by the ultrasonication of diluted graphite oxide dispersion using a Brandson Digital Sonifier (S450D, 500 W, 30 % amplitude) for 30 min. The resulting brown dispersion was then subjected to 20 min of centrifugation at 3,000 rpm to remove any unexfoliated graphite oxide. The GO powder was collected by lyophilization for further characterization and experiments.

Supporting Results

Table S1. Nitrogen adsorption analysis results of different GD_x-T materials

Samples	BET surface area ($m^2\ g^{-1}$)	Pore Volume ($cm^3\ g^{-1}$)	Pore Size (nm)
GD_5-700	143.7	0.12	4.5
GD_5-800	240.5	0.27	4.6
GD_5-900	272.3	0.28	3.9
GD_5-1000	64.8	0.06	6.1
$GD_{2.5}$-900	70.8	0.09	5.0
GD_{10}-900	38.4	0.04	4.3

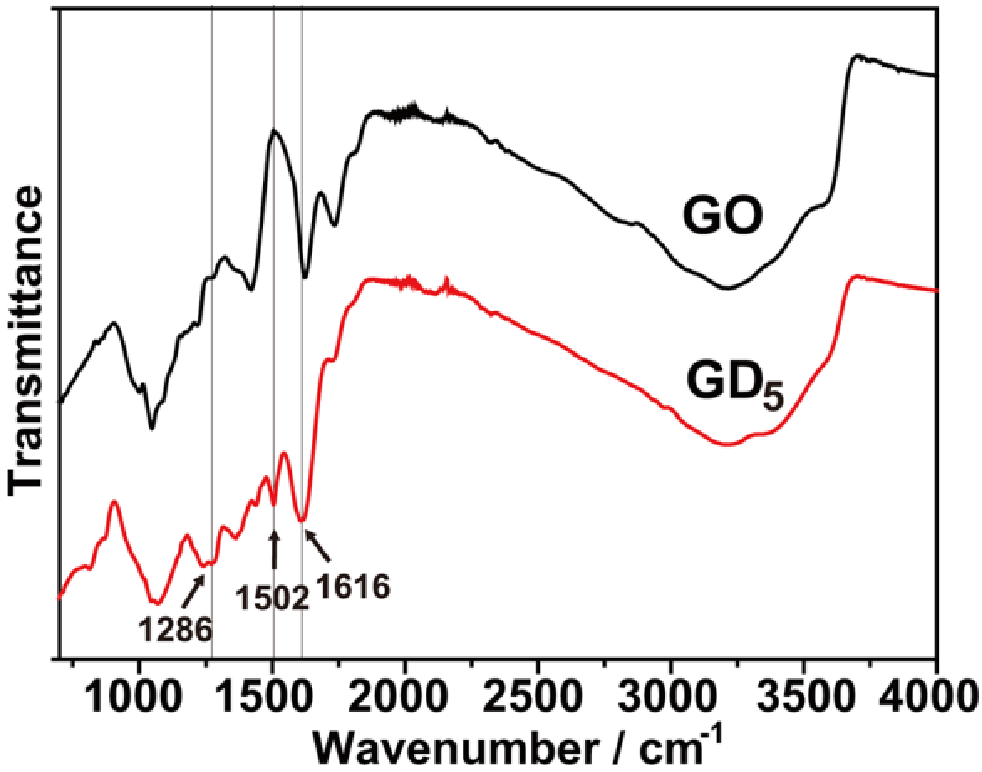

Figure S1. FTIR spectra of GO and GD_5.

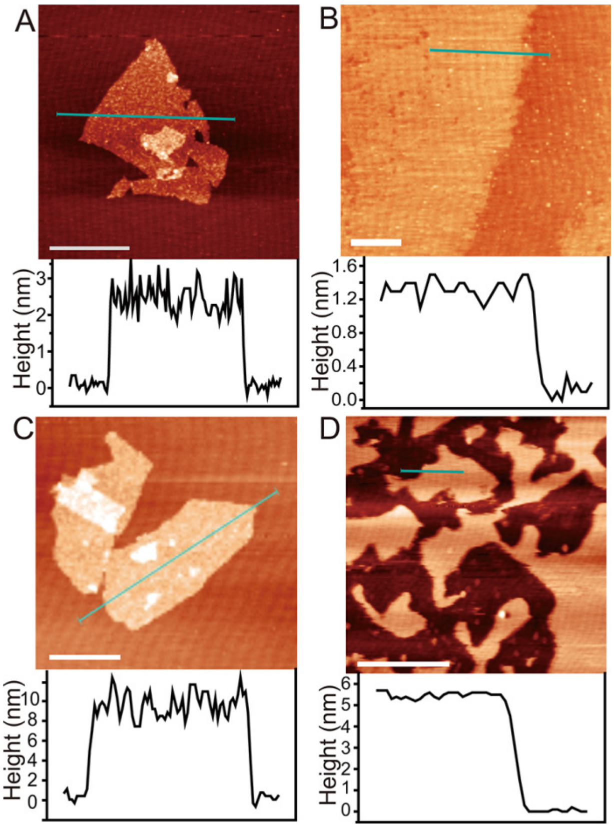

Figure S2. AFM images of (A) $GD_{2.5}$, (B) $GD_{2.5}$-900, (C) GD_{10} and (D) GD_{10}-900, scale bar: 500 nm.

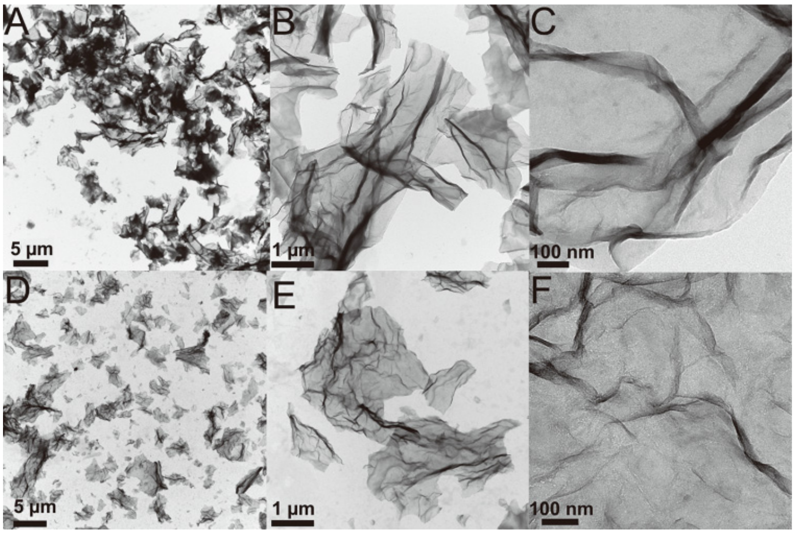

Figure S3. TEM images of (A-C) $GD_{2.5}$-900 and (D-F) GD_{10}-900 at different magnifications.

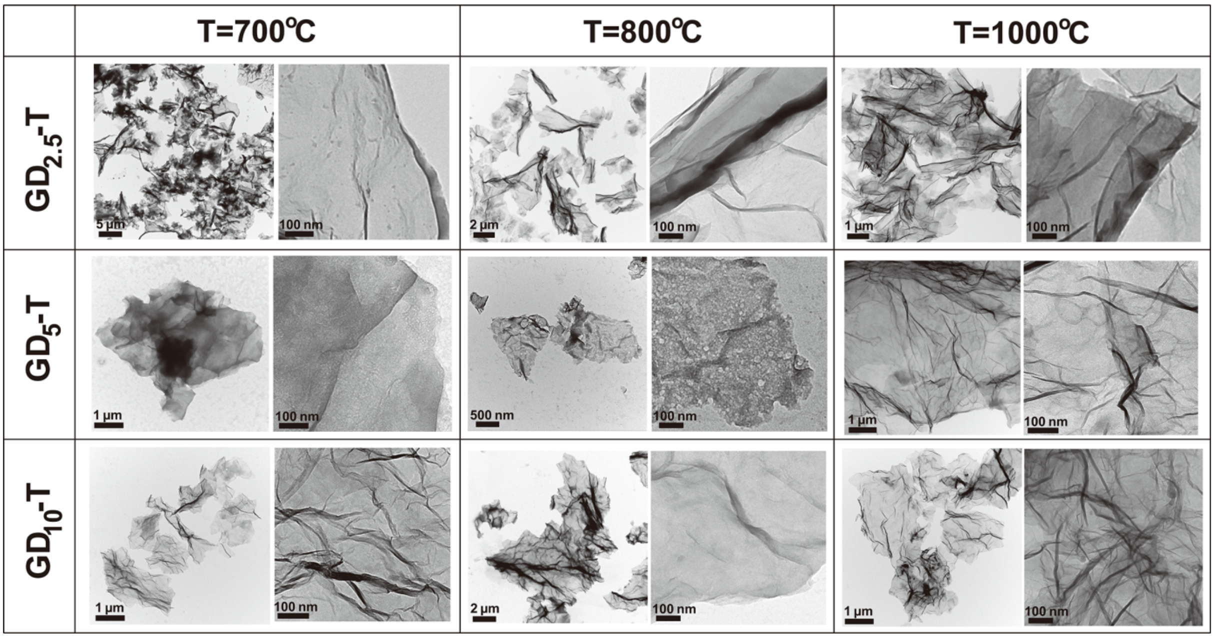

Figure S4. TEM images of GD_x-T materials.

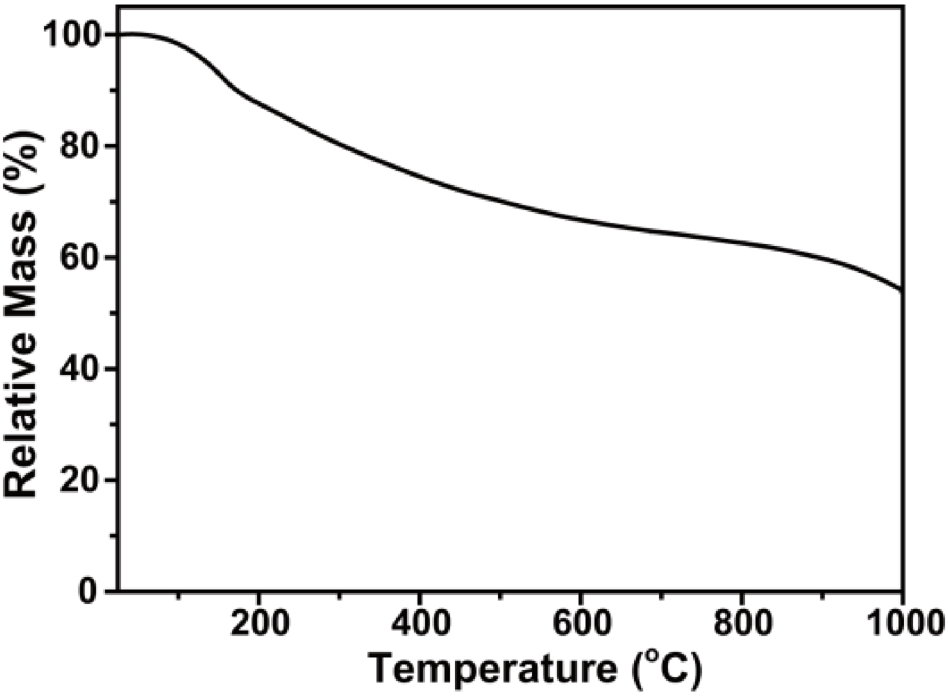

Figure S5. TGA thermogram of GD_5.

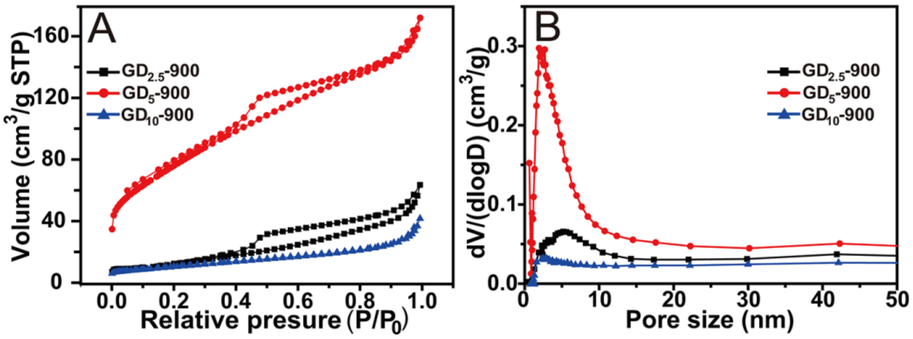

Figure S6. (A) nitrogen adsorption-desorption isotherms and (B) pore size distribution curves of different GD$_x$-900 materials.

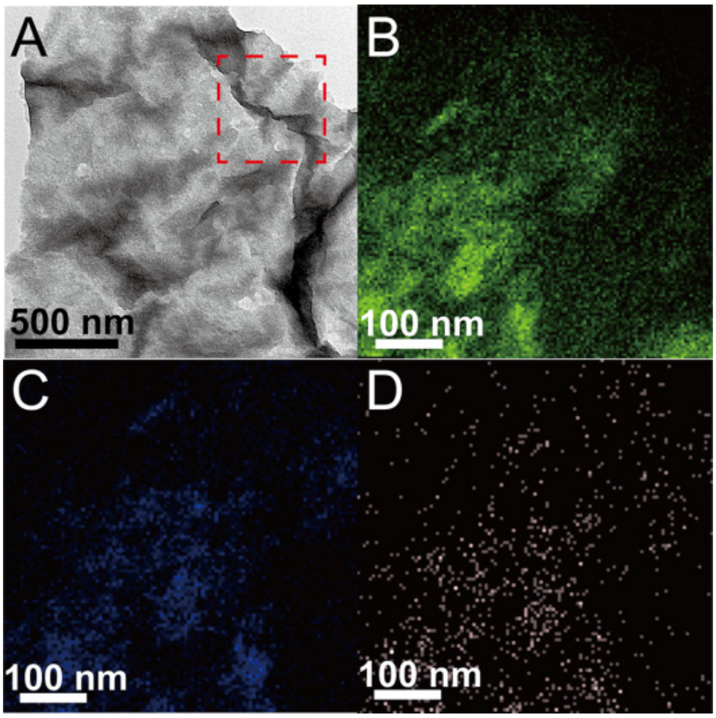

Figure S7. TEM elemental mapping of GD$_5$-900, (A) Bright-field image, (B-D) C, O and N element mapping in the selected square area of A.

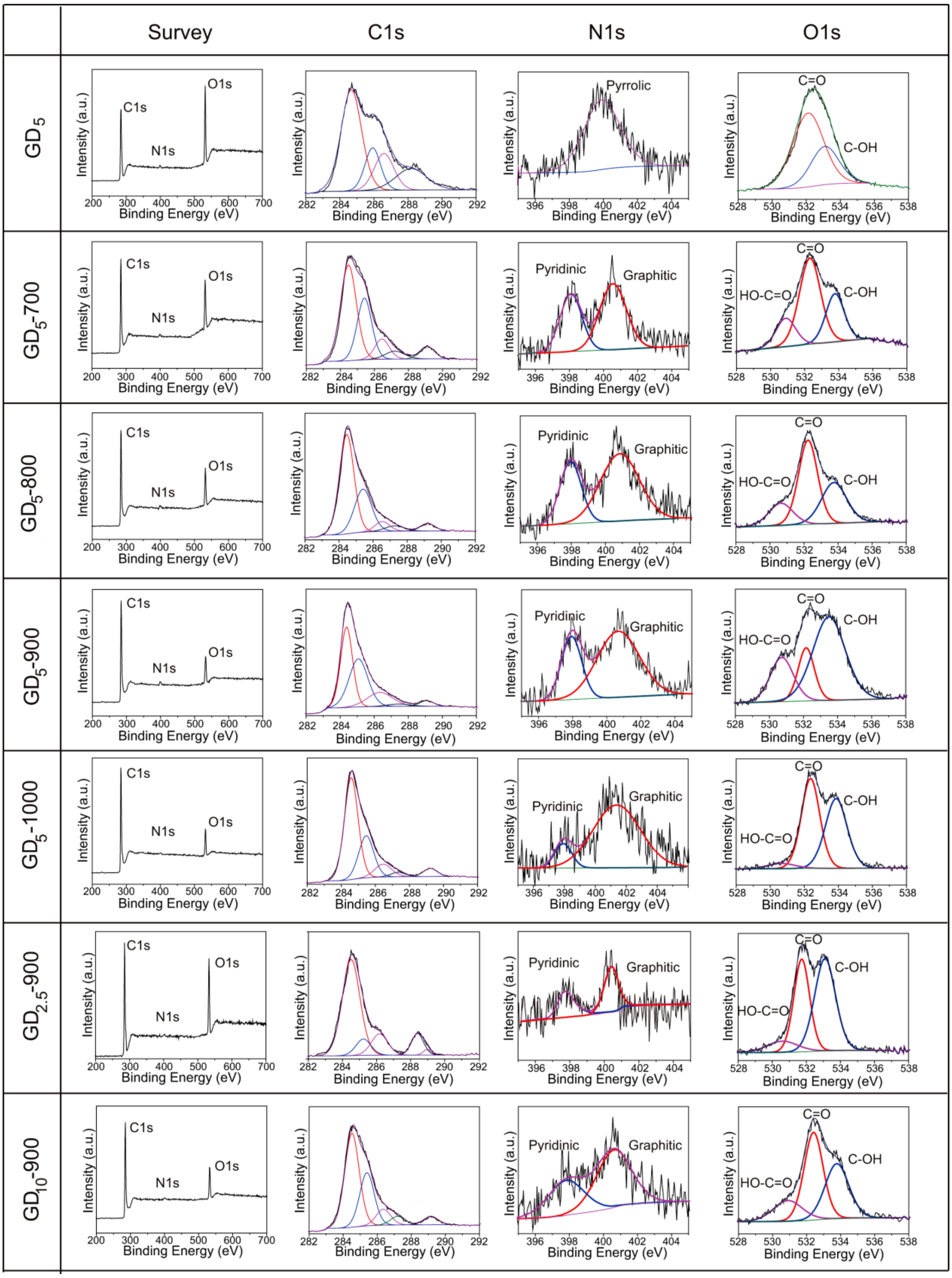

Figure S8. XPS survey spectra, high-resolution spectra of C1s, N1s and O1s of different materials.

For C1s spectra, the main peaks are deconvoluted into five peaks: 284.6 (C=C), 285.4 (C-N/C-H), 286.4 (C-O), 287.3 (C=O) and 289. 1 eV (HO-C=O). For O1s spectra, the main peaks are deconvoluted into three peaks: 530.7 (HO-C=O), 532.1 (C=O) and 533.2 eV (C-OH).

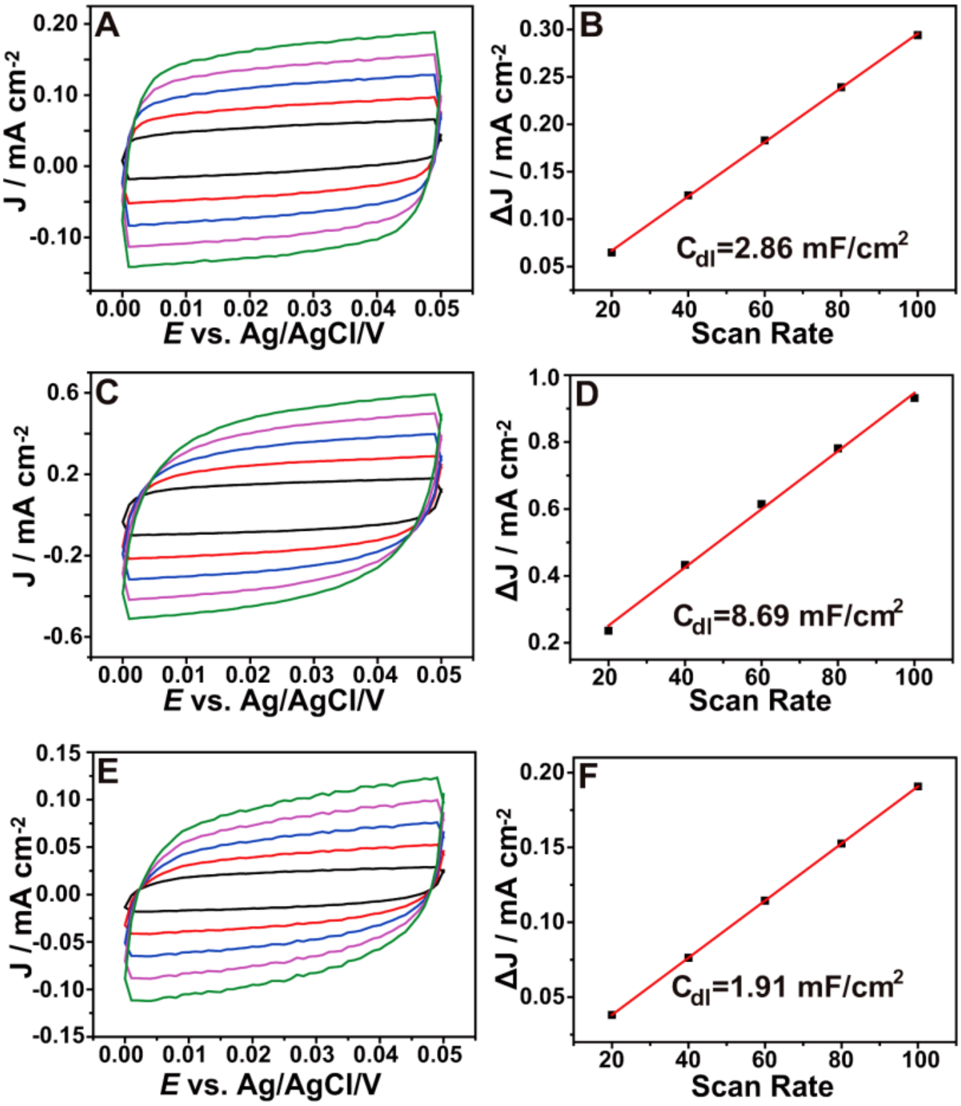

Figure S9. (A, C, E) CV curves and (B, D, F) the corresponding difference in the current density at 0.025 V plotted against scan rate; the calculated C_{dl} values are shown as inset. (A, B): $GD_{2.5}$-900, (C, D): GD_{5}-900, (E, F): GD_{10}-900.

The electrochemical active surface areas (ECSA) of different GD_x-900 catalysts were estimated by measuring their electrochemical double layer capacitances (C_{dl}). The C_{dl} value is linearly proportional to the electrochemical active surface area of the electrode. A potential range of 0.00-0.05 V vs. Ag/AgCl is selected for the capacitance measurements because no obvious electrochemical features corresponding to Faradic current are observed in this region for all catalysts (Figure S9 A, C, E). The capacitive currents, i.e. $\Delta J_{|Ja-Jc|}$ @0.025 V are plotted as a function of CV scan rate, as shown in Figure S9 B, D, F; linear relationships are observed with the slope twice larger than the C_{dl} values. The C_{dl} values for GD_x-900 (x=2.5, 5 and 10) are found to be to 2.86, 8.69, 1.91 mF/cm^2. The observed trend of the ECSA and thickness is similar to that obtained from BET data.

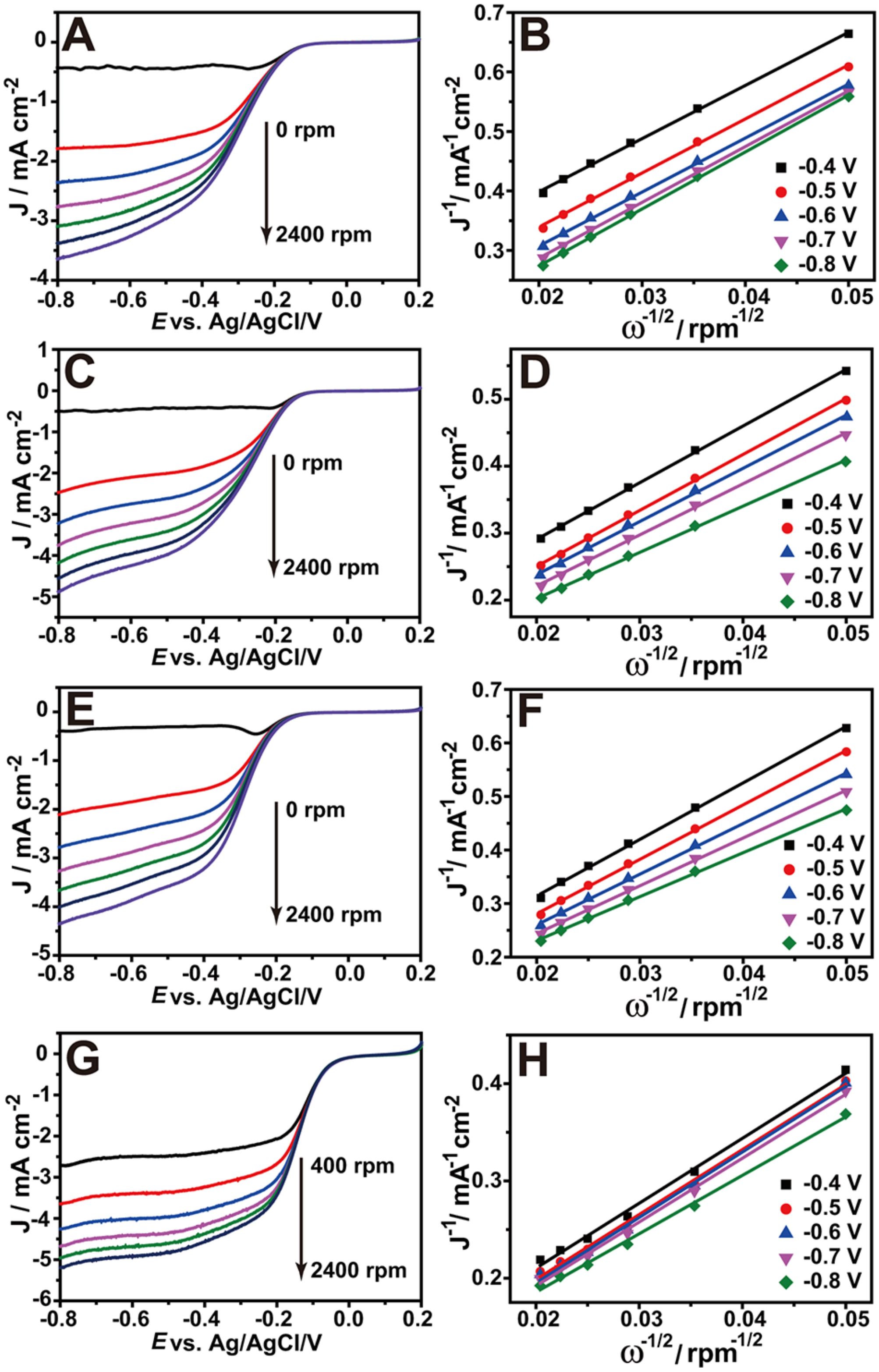

Figure S10. (A, C, E and G) LSVs at different rotating speeds from 0 to 2400 rpm with an increment of 400 rpm between each voltammogram and (B, D, F and H) K-L plots obtained at different potentials: -0.4, -0.5, -0.6, -0.7 and -0.8V. (A, B): GD$_{2.5}$-900, (C, D): GD$_5$-900, (E, F): GD$_{10}$-900 and (G, H): Pt/C

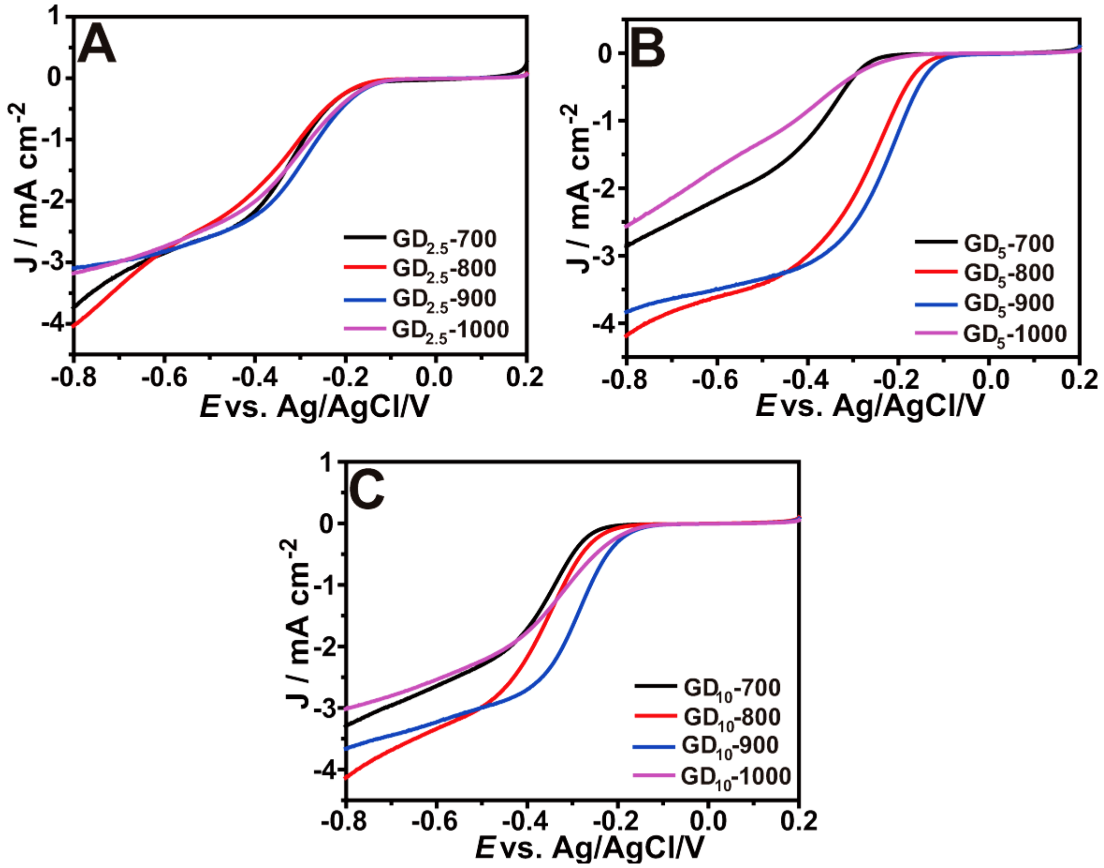

Figure S11. LSVs of different GD$_x$-T materals.